


# Extracellular lipidome change by an SGLT2 inhibitor, luseogliflozin, contributes to prevent skeletal muscle atrophy in *db/db* mice

Ryo Bamba<sup>1</sup> , Takuro Okamura<sup>1</sup>, Yoshitaka Hashimoto<sup>1</sup>, Saori Majima<sup>1</sup>, Takafumi Senmaru<sup>1</sup>, Emi Ushigome<sup>1</sup>, Naoko Nakanishi<sup>1</sup>, Mai Asano<sup>1</sup>, Masahiro Yamazaki<sup>1</sup>, Hiroshi Takakuwa<sup>2</sup>, Masahide Hamaguchi<sup>1</sup> & Michiaki Fukui<sup>1\*</sup>

<sup>1</sup>Department of Endocrinology and Metabolism, Kyoto Prefectural University of Medicine, Kyoto, Japan; <sup>2</sup>Agilent Technologies, Chromatography Mass Spectrometry Sales Department, Life Science and Applied Markets Group, Tokyo, Japan

## Abstract

**Background** Diabetes mellitus increases the excretion of urinary glucose from the renal glomeruli due to elevated blood glucose levels. In the renal tubules, SGLT2 is expressed and reabsorbs the excreted urinary glucose. In the pathogenesis of diabetes mellitus, glucose reabsorption by SGLT2 is increased, and SGLT2 inhibitors improve hyperglycaemia by inhibiting this reabsorption. When urinary glucose excretion is enhanced, glucose supply to skeletal muscle may be insufficient and muscle protein catabolism may be accelerated. On the other hand, SGLT2 inhibitors not only ameliorate hyperglycaemia but also improve fatty acid metabolism in muscle, which may prevent muscle atrophy.

**Methods** Eight-week-old male *db/m* mice or *db/db* mice were fed a standard diet with or without the SGLT2i luseogliflozin (0.01% w/w in chow) for 8 weeks. Mice were sacrificed at 16 weeks of age, and skeletal muscle and serum lipidomes, as well as skeletal muscle transcriptome, were analysed.

**Results** Administration of SGLT2i led to not only decreased visceral fat accumulation ( $P = 0.004$ ) but also increased soleus muscle weight ( $P = 0.010$ ) and grip strength ( $P = 0.0001$ ). The levels of saturated fatty acids, especially palmitic acid, decreased in both muscles ( $P = 0.017$ ) and sera ( $P = 0.041$ ) upon administration of SGLT2i, while the content of monosaturated fatty acids, especially oleic acid, increased in both muscle ( $P < 0.0001$ ) and sera ( $P = 0.009$ ). Finally, the accumulation of transcripts associated with fatty acid metabolism, such as *Scd1*, *Fasn*, and *Elovl6*, and of muscle atrophy-associated transcripts, such as *Foxo1*, *Mstn*, *Trim63*, and *Fbxo32*, decreased following SGLT2i administration.

**Conclusions** Intramuscular fatty acid metabolism and gene expression were influenced by the extracellular lipidome, which was modified by SGLT2i. Hence, secondary effects, other than the hypoglycaemic effects of SGLT2i, might lead to the alleviation of sarcopenia.

**Keywords** SGLT2 inhibitor; Sarcopenia; Muscle atrophy; Lipidome; Transcriptome

Received: 28 October 2020; Revised: 18 August 2021; Accepted: 4 September 2021

\*Correspondence to: Dr. Michiaki Fukui, Department of Endocrinology and Metabolism, Kyoto Prefectural University of Medicine, Graduate School of Medical Science, 465, Kajii-cho, Kamigyo-ku, Kyoto City, Kyoto 621-8585, Japan. Phone: +81-75-251-5505; Fax: +81-75-252-3721, Email: michiaki@koto.kpu-m.ac.jp

## Introduction

The number of patients with diabetes worldwide is on the rise.<sup>1</sup> In response to this situation, a breakthrough for treatment of diabetes has been achieved in recent years with

the introduction of new drugs. For example, sodium glucose cotransporter 2 inhibitors (SGLT2is) selectively inhibit the Na<sup>+</sup>/glucose transporter SGLT2, responsible for glucose reabsorption in proximal renal tubules, thereby increasing urinary excretion of glucose and thus exerting a hypoglycaemic

effect and leading to weight loss.<sup>2</sup> In addition to their hypoglycaemic effects, SGLT2i have been shown to exert secondary effects, through which they reduce the risk of cardiovascular disease, heart failure, and loss of kidney function.<sup>3,4</sup>

Although their weight loss effect is a major benefit, there have been reports of a reduction in lean weight as well as fat weight upon SGLT2i administration.<sup>5,6</sup> Most of the lean body volume loss was due to skeletal muscle volume loss; thus, a concern for the use of SGLT2i is that they might lead to sarcopenia in diabetic patients.<sup>7</sup> However, we have previously shown the potential benefit of SGLT2i against sarcopenia in an animal model of diabetes.<sup>8</sup> Furthermore, previous reports have shown that high concentrations of intracellular fatty acids impair muscular glucose metabolism.<sup>9–11</sup> In addition, intramuscular fatty acid accumulation is thought to increase in patients with sarcopenia or sarcopenic obesity.<sup>12</sup> On the other hand, SGLT2i are thought to decrease intramuscular as well as extracellular fatty acid accumulation. However, the mechanism by which SGLT2i influence fatty acid metabolism in skeletal muscle has not been elucidated to date. Here, we investigated the preventive effect of SGLT2 inhibitors on muscle atrophy based on fatty acid dynamics in skeletal muscle by animal and cell experiments.

## Materials and methods

### Mice and experimental design

All experimental procedures were approved by the Committee for Animal Research, Kyoto Prefectural University of Medicine. C57BLKS/J *lar-Lepr<sup>db</sup>/Lepr<sup>db</sup>* mice (*db/db* mice) and C57BLKS/J *lar-m/lepr<sup>db</sup>* mice (*db/m* mice) were housed in the Kyoto Prefectural University of Medicine Animal Facility (M2020-38). Eight-week-old male non-diabetic heterozygous *db/m* mice and 8-week-old male diabetic homozygous *db/db* mice were purchased from Shimizu Laboratory Supplies (Kyoto, Japan). The mice were fed a normal diet (4 kcal/g, fat kcal 16%; EP Trading Co., Ltd, Tokyo, Japan) (Table 1) for 8 weeks starting at 8 weeks of age. The mice were divided into the following four groups and the following experiments were performed with six mice in each group: (i) *db/m* mice without SGLT2i (*db/m*), (ii) *db/m* mice with SGLT2i, (iii) *db/db* mice without SGLT2i (*db/db*), and (iv) *db/db* mice with SGLT2i. In this study, luseogliflozin [Lusefi® (Japan)], which is an orally active second-generation SGLT2 inhibitor developed by Taisho Pharmaceutical Co., Ltd for the treatment of patients with type 2 diabetes mellitus, was used. Luseogliflozin was mixed with the chow at a ratio of 0.01% per weight, which was the same dose as our previous study.<sup>8</sup> At 16 weeks of age, all mice were sacrificed via administration of a combination of anaesthetics: 0.3 mg/kg

**Table 1** Composition of nutrients in feed

	Weight ratio	Calorie ratio
Protein	20	20
Carbohydrates	64	64
Fat	7	16
Total		100
kcal/g	4	
Using raw materials	g	kcal
Casein	200	800
DL-Methionine	0	0
L-Cystine	3	12
Com starch	397.486	1590
Maltodextrin	132	528
Sucrose	100	400
Cellulose	50	0
Corn oil	0	0
Soybean oil	70	630
t-Butylhydroquinone	0.014	0
Mineral mix S10001	0	0
Mineral mix S10022G	35	0
Mineral mix S10022M	0	0
Vitamin mix V10001	0	0
Vitamin mix V10037	10	40
Choline bitartrate	2.5	0
Total	1000	4000

of medetomidine, 4.0 mg/kg of midazolam, and 5.0 mg/kg of butorphanol (Figure 1A).<sup>13</sup> Liver, epididymal fat, soleus, and plantaris muscle weights were obtained and normalized by body weight, respectively.

### Fasting blood glucose levels and glucose tolerance tests

Fourteen-hour fasting blood glucose levels were investigated at 10, 12, 14, and 16 weeks old. Insulin tolerance test (ITT) (0.5 U/kg) (six animals per group, 3 days before sacrifice) and intraperitoneal glucose tolerance test (iPGTT) (1 mg/g) (2 days before sacrifice) were performed in 16-week-old mice that had been fasted for 5 and 14 h, respectively, and the area under curve was evaluated. Blood glucose levels were measured from the tail vein using a glucometer (Gultest mintII; Sanwa Kagaku Kenkyusho, Nagoya, Japan). The iPGTT and ITT results were analysed by measuring the area under the curve (AUC).

### Biochemistry

Blood samples were taken from fasted mice, and aspartate aminotransferase (AST), alanine aminotransferase (ALT) levels, total cholesterol, triglycerides (TGs), and non-esterified fatty acids (NEFA) were measured. The biochemical examinations were performed at FUJIFILM Wako Pure 18 Chemical Corporation (Osaka, Japan).

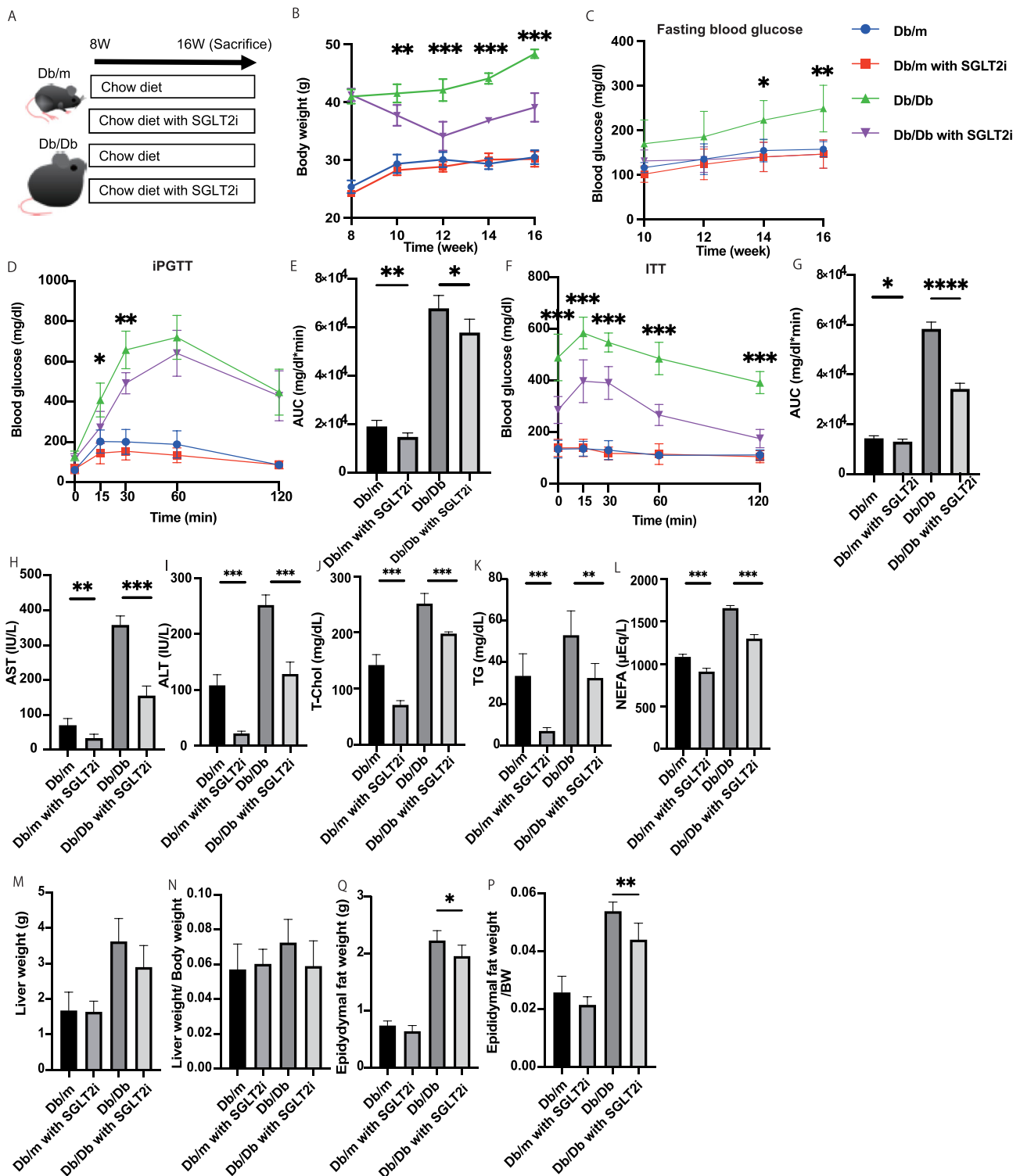


**Figure 1** Treatment of *db/db* mice with SGLT2i decreases body weight, blood glucose levels, and hepatic enzyme, and serum lipid levels. (A) Outline of the feeding and sacrifice protocol ( $n = 6$ ). (B) Body weight change ( $n = 6$ ).  $**P < 0.01$ , and  $***P < 0.001$  significant difference between Db/Db mice and Db/Db mice with SGLT2i at the respective weeks. (C) Fasting blood glucose ( $n = 6$ ).  $*P < 0.05$ ,  $**P < 0.01$  significant difference between Db/Db mice and Db/Db mice with SGLT2i at the respective weeks. (D) Intraperitoneal glucose tolerance test (iPGTT) (1 mg/g) results ( $n = 6$ ).  $*P < 0.05$ ,  $**P < 0.01$  significant difference between Db/Db mice and Db/Db mice with SGLT2i at the respective times. (E) Area under the iPGTT curve ( $n = 6$ ). (F) Insulin tolerance test (ITT) results.  $***P < 0.001$  significant difference between Db/Db mice and Db/Db mice with SGLT2i at the respective times. (G) Area under the ITT curve ( $n = 6$ ). (H) Serum aspartate aminotransferase (AST) concentration ( $n = 6$ ). (I) Serum alanine aminotransferase (ALT) concentration ( $n = 6$ ).

(J) Serum total cholesterol (T-Chol) concentration ( $n = 6$ ). (K) Serum triglyceride (TG) concentration ( $n = 6$ ). (L) Serum non-esterified fatty acid (NEFA) concentration ( $n = 6$ ). (M, N) Absolute and relative liver weight ( $n = 6$ ). (O, P) Absolute and relative weight of epididymal fat ( $n = 6$ ). Data are presented as mean  $\pm$  standard deviation. \* $P < 0.05$ , \*\* $P < 0.01$ , \*\*\* $P < 0.001$ , and \*\*\*\* $P < 0.0001$  using Tukey's honestly significant difference test.

### Grip strength assay

Grip strength was measured using a grip strength metre for mice (model DS2-50N, IMADA Co., Ltd, Toyoashi, Japan) on another batch of 16-week-old mice. We performed six consecutive measurements per day at 1 min intervals, and the investigators did not know which mice were in which group. In addition, grip strength was normalized to body weight.

### Liver histology

Liver tissue was obtained and fixed with 10% buffered formaldehyde or embedded in paraffin. Tissue sections were prepared and stained with haematoxylin and eosin (HE) and Masson's Trichrome (MT) stains. Additionally, the non-alcoholic fatty liver disease (NAFLD) activity score (NAS) was adopted to assess NAFLD severity.<sup>14</sup> The NAS was evaluated by a trained hepatopathologist while masking the experimental conditions. Briefly, the scoring system consisted of 14 histological features, four of which were evaluated semiquantitatively: hepatocellular ballooning (0–2), lobular inflammation (0–2), steatosis (0–3), and fibrosis (0–4). In addition, to assess fibrosis, Stage 1 was classified as follows: 1A, mild pericentral perisinusoidal fibrosis; 1B, moderate or greater perisinusoidal fibrosis; and 1C, fibrosis in the portal region or periportal vein. Perisinusoidal or periportal fibrosis was classified as Stage 2, bridging fibrosis as Stage 3, and liver cirrhosis as Stage 4. Images were captured with a fluorescence microscope BZ-X710 (Keyence, Osaka, Japan).

### Quantification of free fatty acids in the soleus muscle, sera, and liver

The composition of fatty acids in the soleus muscle tissue, sera, and liver tissue of *db/m* mice, *db/m* mice with SGLT2i, *db/db* mice, and *db/db* mice with SGLT2i was measured using gas chromatography–mass spectrometry (GC–MS) with an Agilent 7890B/7000D instrument (Agilent Technologies, Santa Clara, CA, USA). Fifteen milligrams of liver tissue and 25  $\mu$ L of sera were methylated using a fatty acid methylation kit (Nacalai Tesque, Kyoto, Japan). If the sample weight was less than 15 mg, the concentration was calculated by dividing by the weight. The final product was loaded onto a Varian capillary column (DB-FATWAX UI; Agilent Technologies). The CP-Sil 88 for FAME capillary column was used for fatty acid separation (100 m  $\times$  an inner diameter of 0.25 mm  $\times$  membrane thickness of 0.20  $\mu$ m; Agilent Technologies). The column temperature was maintained at 100°C for

4 min and then increased gradually by 3°C/min to 240°C and held for 7 min. The sample was injected in split mode with a split ratio of 5:1. Each fatty acid methyl ester was detected in the selected ion monitoring mode. All results were normalized to the peak height of the C17:0 internal standard.<sup>15</sup>

### Next-generation sequencing and quantitative RT–PCR

Next-generation sequencing was performed using a NovaSeq 6000 platform at MacroGen Japan Corp. (Tokyo, Japan). Libraries for RNA-seq were prepared using the TruSeq Stranded mRNA LT Sample Prep Kit (Illumina, San Diego, CA, USA), and fragments per kilobase of exon per million mapped reads (FPKM) were calculated for RefSeq\_2017\_06\_12 for expression analysis.

Next, the relative mRNA abundance within the groups was evaluated through the weighted average distance (WAD) method using R<sup>16</sup> and unpaired *t*-tests. The WAD method ranked the genes based on higher expression, higher weights, or fold change. WAD was found to be an effective method for transcriptome analysis. Then, the  $\log_2(\text{FPKM} + 1)$  of the top 30 genes was visualized in heat maps.<sup>17</sup>

Data were preprocessed by Robust Multichip Average (RMA) normalization, and the global gene expression was visualized as a volcano plot.

Among the identified genes, the expression of *Scd1* was analysed with quantitative RT–PCR. Each muscle and liver sample was homogenized in ice-cold QIAzol Lysis reagent (Qiagen, Hilden, Germany), and total RNA was isolated with RNeasy MinElute Cleanup Kit (Qiagen) as described in the manufacturer's instructions. Total RNA (0.5  $\mu$ g) was reverse-transcribed using a High-Capacity cDNA Reverse Transcription Kit (Applied Biosystems, Foster City, CA, USA) for first-strand cDNA synthesis, using an oligonucleotide dT primer and random hexamer primers according to the manufacturer's recommendations. The reverse transcription reaction was performed for 120 min at 37°C, and the enzyme was then inactivated by incubation at 85°C for 5 min. RT–PCR was performed using TaqMan Fast Advanced Master Mix (Applied Biosystems) according to the manufacturer's instructions. The following PCR conditions were used: one cycle of 2 min at 50°C and 20 s at 95°C, followed by 40 cycles of 1 s at 95°C and 20 s at 60°C.

Total RNA extracted from muscle and liver was diluted to 5 ng/ $\mu$ L for all samples in DNase-RNase free water after concentration measurement by Thermo Scientific™ NanoDrop Lite (Thermo Scientific Waltham, MA, USA). The

relative expression level of each target gene was normalized to the *Gapdh* threshold cycle (CT) value and quantified using the comparative threshold cycle  $2^{-\Delta\Delta CT}$  method as previously described.<sup>18</sup> Additionally, the experiments using *Pak1ip1* and *18s* for normalization were performed. Signals from *db/m* mice were assigned a relative value of 1.0. Six mice from each group were examined, and RT-PCR was run in triplicate for each sample.

### *Immunocytochemistry of murine soleus muscle*

Soleus muscle biopsies were fixed in a 10% formalin solution and embedded in paraffin. Muscle sections were prepared and stained with monoclonal primary anti-MuRF1 antibodies (C-11, sc-398608, <https://www.scbt.com/ja/p/murf1-antibody-c-11>, Santa Cruz Biotechnology, Santa Cruz, CA, USA),<sup>19</sup> followed by a Texas-red-conjugated anti-mouse secondary antibody (Jackson ImmunoResearch, West Grove, PA, USA). Nuclei were stained with 4',6-diamidino-2-phenylindole (DAPI) (Sigma-Aldrich, St. Louis, MO, USA). Images were captured with a BZ-X710 fluorescence microscope (Keyence, Osaka, Japan), and analysis of the fluorescence intensity of myotube cells were carried out using the ImageJ software [National Institutes of Health (NIH)]. Moreover, images of negative control were prepared in all of the conditions.

### *Protein extracts and western blot incubated with antibodies*

Soleus muscle of both legs was homogenized and extracted in a radio immunoprecipitation assay buffer [RIPA, ATTO, Tokyo; 50 mmol/L Tris (pH 8.0), 150 mmol/L NaCl, 0.5% deoxycholate, 0.1% sodium dodecyl sulfate (SDS), and 1.0% NP-40] containing a protease inhibitor cocktail (BioVision, Milpitas, CA, USA). Protein assays were performed using a bovine serum albumin (BSA) protein assay kit (Pierce/Thermo Scientific, Rockford, IL, USA) according with the manufacturer's instructions. Total protein was electrophoresed in 12% sodium dodecyl sulfate-polyacrylamide gel electrophoresis (SDS-PAGE) gels, and western blotting was carried out using standard protocols and proteins detected by ImageQuant LAS 500 (GE Healthcare, Piscataway, NJ, USA).

First, 40–60 µg of protein extraction were incubated with the following primary antibodies: monoclonal primary anti-MuRF1 antibodies (1:500) or *gapdh* (1:1500) diluted with EzBlock Chemi (ATTO, Osaka, Japan) overnight at 4°C, followed by incubation with goat anti-mouse IgG secondary antibodies conjugated to horseradish peroxidase diluted with EzBlock Chemi for 30 min at room temperature. The protein expression levels were quantified by optical density using ImageJ (NIH). All the antibodies listed in this section were obtained from Santa Cruz Biotechnology (Santa Cruz).

### *Mouse skeletal muscle cell culture*

Mouse myoblasts (cell line C2C12, KAC Co., Ltd., Kyoto, Japan) were seeded on 24-well plates and grown in Dulbecco's modified Eagle's medium (DMEM) supplemented with 20% foetal bovine serum (FBS) (Day 2). The medium was changed every other day. When the cells reached 80% confluence, their differentiation was induced with DMEM supplemented with 2% horse serum (differentiation medium) (Day 0). C2C12 myotube cells were treated with 100 µM of palmitic acid, while control cells were treated with 100% ethanol of the same volume as the palmitic acid solution for 96 h. After 96 h (Day 5), we subjected the myotube cells to several assays.

### *Immunocytochemistry of C2C12 myotube cells*

C2C12 myotube cells were cultured in eight-well chamber slides, and immunocytochemistry was performed on Day 5. The myotube cells were fixed in 4% paraformaldehyde and incubated overnight at 4°C with the following primary monoclonal antibodies: MY32 against myosin heavy chain (Sigma-Aldrich) or monoclonal primary anti-MuRF1 antibodies (Santa Cruz Biotechnology, Santa Cruz, CA, USA) diluted in phosphate buffered saline (PBS) with 1% BSA and 0.3% Triton™ X-100 (Sigma-Aldrich); next, the samples were incubated with a Texas-red-conjugated anti-mouse secondary antibody diluted in PBS with 1% BSA and 0.3% Triton™ X-100 at 4°C for 1 h. Nuclei were stained with DAPI. Images were captured with a BZ-X710 fluorescence microscope, and analysis of the fluorescence intensity of myotube cells and cell nuclei count per image were carried out using ImageJ. In addition, the fusion index was defined and determined according to a previous study.<sup>20</sup> Briefly, fusion index is an index of differentiation obtained by measuring the ratio of the number of nuclei in myotubes to the total number of nuclei in each field of view. Moreover, the incorporation of a secondary antibody control of immunostaining was performed in all of the conditions.

### *Protein extracts and western blot incubated with antibodies of C2C12 myotube cells*

C2C12 myotube cells were subjected to protein extractions. First, 40–60 µg of protein extraction were incubated with the following primary antibodies: MuRF-1 (1:500), MY32 (1:500), or *gapdh* (1:1500) diluted with EzBlock Chemi (ATTO, Osaka, Japan) overnight at 4°C, followed by incubation with goat anti-mouse IgG secondary antibodies conjugated to horseradish peroxidase diluted with EzBlock Chemi for 30 min at room temperature. All the antibodies listed in this



section were obtained from Santa Cruz Biotechnology (Santa Cruz, Dallas, TX, USA).

### Gene expression in C2C12 myotube cells

Gene expression in C2C12 myotube cells was analysed on Day 5. We removed the medium and washed the cells with cold PBS twice. Cells were detached using cell scrapers and homogenized in ice-cold QIAzol Lysis reagent. The subsequent procedure was the same as that described in the Next-generation sequencing and quantitative RT-PCR section. We performed RT-PCR to quantify the following: *Foxo1*, *Mstn*, *Hdac4*, *Trim63*, *Fbxo32*, *Scd1*, *Fasn*, *Srebf1*, *Elovl6*, *Il6*, and *Bax* mRNA expression levels in the C2C12 myotube cells.

### Statistical analysis

The data were analysed using the JMP software Version 13.0 (SAS, Cary, NC, USA). Differences between two groups were assessed using the unpaired *t*-test and that differences between more than three groups were assessed using Tukey's honestly significant difference test. *P*-values of 0.05 were considered statistically significant. Figures were generated using the GraphPad Prism software Version 8.0 (San Diego, CA, USA).

## Results

### Experimental design

Eight-week-old male *db/m* mice were used as the control group and were housed for 8 weeks in a different cage at the same time as *db/db* mice of the same age. The *db/m* and *db/db* mice were divided into two groups: *db/m* or *db/db* with SGLT2i group that was fed a 0.01% luseogliflozin-supplemented diet and *db/m* or *db/db* without SGLT2i group that was fed a standard chow diet. Experiments were conducted with six animals for each group. Paired feeding was performed by supplying the same amount of feed. An overview of the experimental design is shown in Figure 1A.

### Effect of SGLT2i on body weight and glucose homeostasis

After the 8-week dietary treatment, the body weight of *db/db* mice was significantly greater than that of *db/m* mice. The body weight of *db/m* mice treated with SGLT2i was not different from that without; on the other hand, the body weight of

*db/db* mice treated with SGLT2i was significantly lower than that of *db/db* mice (Figure 1B).

The fasting blood glucose levels were not different between *db/m* mice with and without SGLT2i; on the other hand, the fasting blood glucose of *db/db* mice without SGLT2i increased with age, and from 14 weeks, the fasting blood glucose levels in *db/db* mice were higher with statistical significance (Figure 1C). The results of iPGTT and ITT of *db/db* mice were significantly worse than those of *db/m* mice; furthermore, the iPGTT and ITT results for *db/db* mice treated with SGLT2i were significantly better compared with those of *db/db* mice (Figure 1D–1G).

### Effect of SGLT2i on serum biochemistry and serum lipid analysis

In *db/db* mice, serum AST and ALT levels were significantly higher than those in *db/m* mice, suggesting that fatty livers developed in *db/db* mice. However, serum ALT levels were diminished in *db/m* and *db/db* mice treated with SGLT2i (Figure 1H and 1I). Similarly, total cholesterol (T-Chol), TG, and NEFA levels significantly increased in *db/db* mice compared with those of *db/m* mice, but they were significantly lowered in *db/m* and *db/db* mice treated with SGLT2i (Figure 1J–1L).

### Effect of SGLT2i on organ weight and non-alcoholic fatty liver disease

The absolute and relative liver weights of *db/db* mice were greater than those of *db/m* mice. On the other hand, the absolute and relative liver weights of *db/db* mice treated with SGLT2i tended to be lower than those of *db/db* mice (Figure 1M and 1N). The hepatic fat accumulation evaluated by NAFLD activity score was significantly lower in *db/m* mice than in *db/db* mice, and that was significantly reduced by SGLT2i in both groups (Supporting Information, Figure S1A and S1B). In addition, fibrosis was also improved by the treatment of SGLT2i in *db/db* mice (Figure S1A and S1C).

Moreover, the absolute and relative weights of epididymal fat in the two groups of *db/db* mice were greater than those of *db/m* mice. However, among *db/db* mice, the absolute and relative weights of epididymal fat in *db/db* mice treated with SGLT2i were significantly lower than those of *db/db* mice (Figure 1O and 1P).

### Effect of SGLT2i on skeletal muscle weight and grip strength

The absolute and relative grip strength of *db/m* and *db/db* mice was significantly lower than those treated with SGLT2i

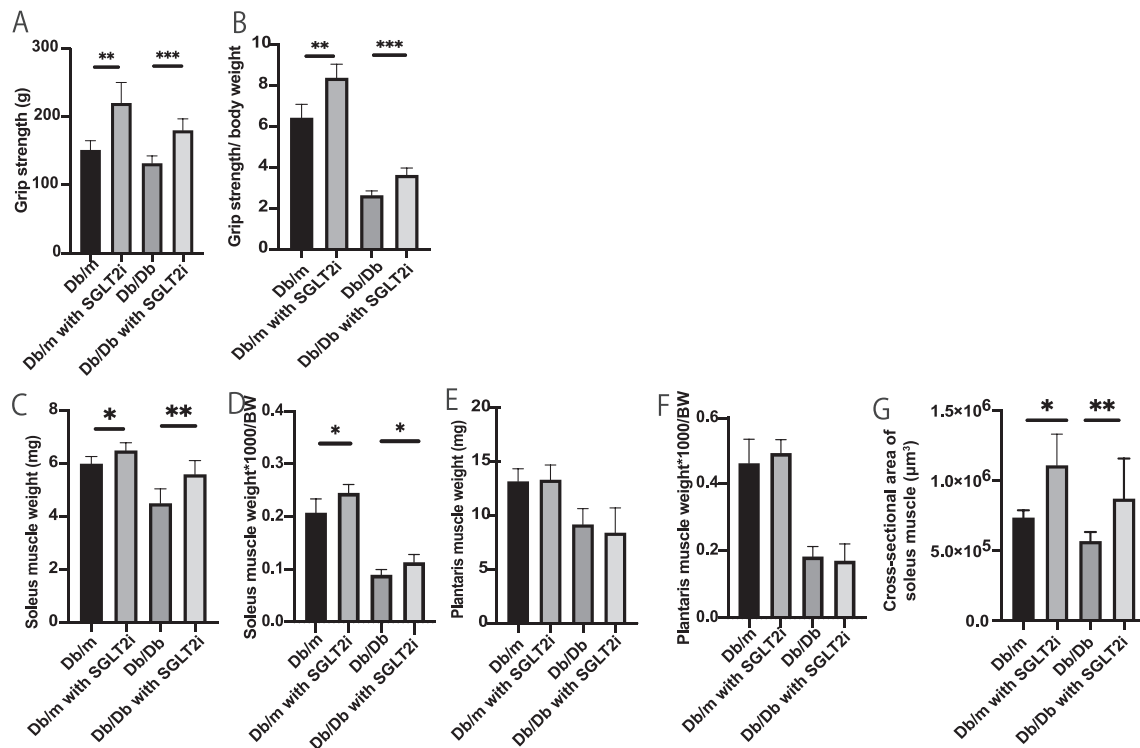


**Figure 2** Treatment of *db/db* mice with SGLT2i increases grip strength and skeletal muscle mass. (A, B) Absolute and relative grip strength ( $n = 6$ ). (C, D) Absolute and relative soleus muscle weight ( $n = 6$ ). (E, F) Absolute and relative plantaris muscle weight ( $n = 6$ ). (G) Cross-sectional area of soleus muscle ( $n = 6$ ). Data are presented as mean  $\pm$  standard deviation. \* $P < 0.05$ , \*\* $P < 0.01$ , and \*\*\* $P < 0.001$ , using Tukey's honestly significant difference test.

(Figure 2A and 2B). Furthermore, in *db/db* mice, the absolute and relative soleus muscle weights were lower than those of *db/m* mice. However, these were significantly increased by SGLT2i treatment of *db/m* and *db/db* mice (Figure 2C and 2D). On the other hand, in *db/db* mice, the absolute and relative plantaris muscle weights were lower than those of *db/m* mice; however, the treatment of SGLT2i did not increase the absolute and relative plantaris muscle weights in *db/m* and *db/db* mice (Figure 2E and 2F). Consistently, the cross-sectional area of soleus muscle of *db/db* mice was increased by SGLT2i administration (Figure 2G).

### Effect of SGLT2i on fatty acid concentrations in muscle, serum, and liver

The levels of lauric acid, myristic acid, and stearic acid, that is, saturated fatty acids, in skeletal muscle significantly increased in *db/db* mice than in *db/m* mice. However, such accumulation was significantly mitigated in *db/db* mice treated with SGLT2i (Figure 3A, 3B, and 3D). In addition, in both muscle and serum, the concentration of palmitic acid was significantly higher in *db/db* mice than in *db/m* mice, while it was significantly improved by SGLT2i treatment (Figure 3C and 3H). On the other hand, the serum levels of oleic acid, a

monounsaturated fatty acid, were significantly decreased in *db/db* mice but were increased by SGLT2i administration. Oleic acid concentrations in skeletal muscle were not significantly different between *Db/m* and *Db/Db* mice but were significantly increased by SGLT2i administration in *Db/Db* mice (Figure 3E and 3J). Additionally, in liver, saturated fatty acids concentration was significantly higher in *db/db* mice than in *db/m* mice, while it was significantly improved by SGLT2i treatment (Figure S1D–S1G). On the other hand, oleic acid concentration in liver was significantly decreased in *db/db* mice but increased upon administration of SGLT2i (Figure S1H).

### Comprehensive analysis of RNA sequencing data

To compare gene expression in skeletal muscles, total RNA was extracted from soleus muscle samples and transcriptome analysis was performed with NGS. Gene expression differed between *db/db* mice and *db/m* mice, as well as between *db/db* mice treated or not with SGLT2i (Figure S2A–S2C).

The expression of genes encoding enzymes, which catalyse reactions in the fatty acid biosynthetic pathway, increased in *db/db* mice compared with that in *db/m* mice but decreased in *db/db* mice treated with SGLT2i (Figure 4A). Particularly

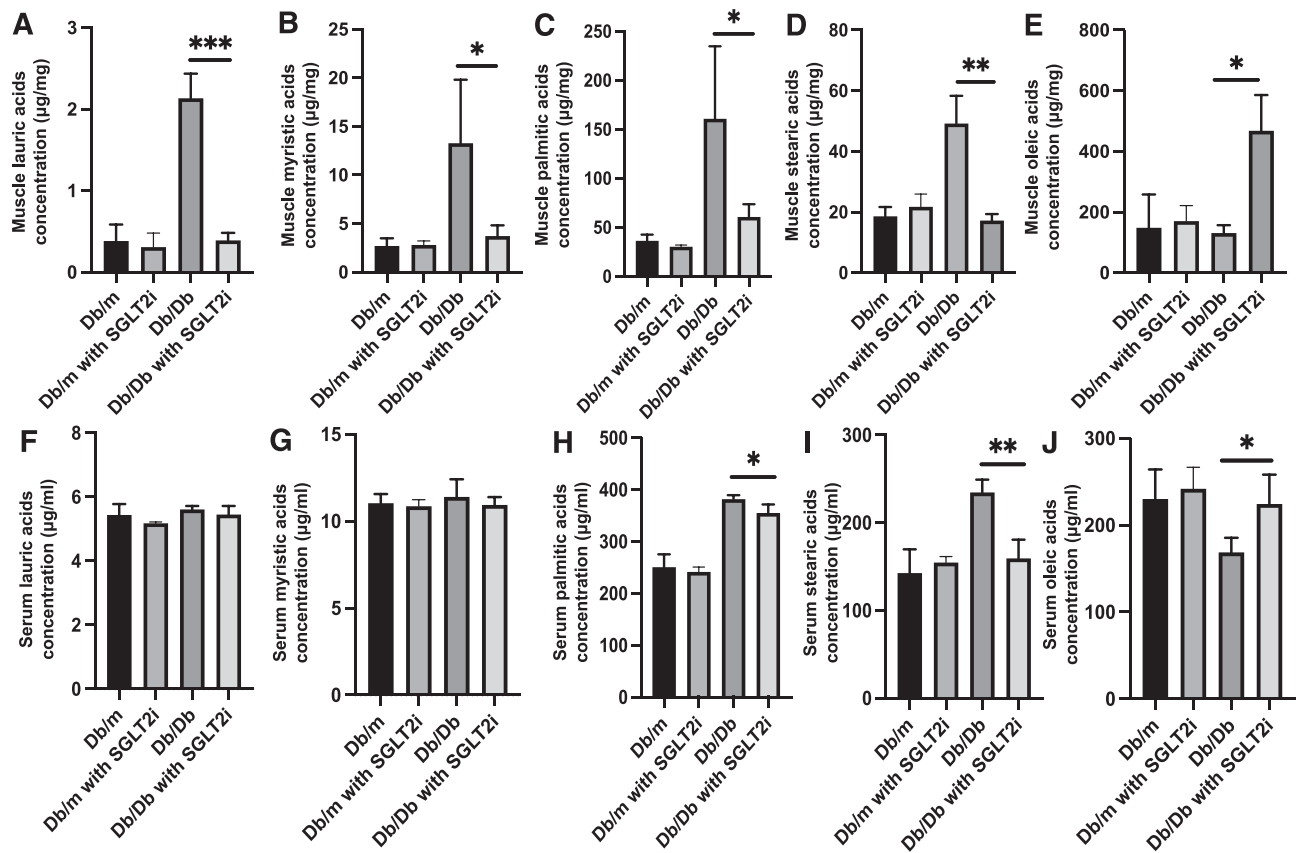


**Figure 3** Treatment of *db/db* mice with SGLT2i decreases the concentration of lauric acid, myristic acid, palmitic acid, and stearic acid whereas increases that of oleic acid in the skeletal. (A) Lauric acid concentrations in muscle ( $n = 6$ ). (B) Myristic acid concentrations in muscle ( $n = 6$ ). (C) Palmitic acid concentrations in muscle ( $n = 6$ ). (D) Stearic acid concentrations in muscle ( $n = 6$ ). (E) Oleic acid concentrations in muscle ( $n = 6$ ). (F) Serum lauric acid concentrations ( $n = 6$ ). (G) Serum myristic acid concentrations ( $n = 6$ ). (H) Serum palmitic acid concentrations ( $n = 6$ ). (I) Serum stearic acid concentrations ( $n = 6$ ). (J) Serum oleic acid concentrations ( $n = 6$ ). Data are presented as mean  $\pm$  standard deviation. \* $P < 0.05$ , \*\* $P < 0.01$ , and \*\*\* $P < 0.001$ , using Tukey's honestly significant difference test.

relevant to this study was stearoyl-CoA desaturase-1 (SCD1). SCD1 is a rate-limiting enzyme that converts saturated fatty acids like palmitate and stearate into monounsaturated fatty acids palmitoleate and oleate.<sup>21</sup> Fold change of *Scd1* mRNA expression in microarray and RT-PCR confirmed that the expression of *Scd1* in soleus muscle of *db/db* mice was significantly higher than that in *db/m* mice. Conversely, the expression of *Scd1* in *db/db* mice treated with SGLT2i was significantly lower than that in *db/db* mice (Figure 4B–4E). Moreover, the expression of *Scd1* in liver of *db/db* mice treated with SGLT2i was significantly lower than that of *db/db* mice (Figure S11).

#### Decreased expression intensity of MuRF1 in soleus muscle tissues under SGLT2i administration

Immunostaining of soleus muscle tissues demonstrated that the fluorescence intensity of MuRF1 (Muscle RING-Finger Protein-1) in *db/db* mice was significantly higher than that

of *db/m* mice, whereas that of *db/db* mice treated with SGLT2i was significantly lower than that of *db/db* mice (Figure 5A and 5B). Moreover, in western blotting, the elevation of MuRF1 protein content occurred in *db/db* mice, compared with that in *db/m* mice, whereas the treatment of SGLT2i decreased the protein content (Figure 5C and 5D).

#### Palmitic acid treatment leads to myotube cell atrophy

We performed immunostaining with monoclonal antibodies for myosin heavy chain and MuRF1 diluted in PBS supplemented with 1% BSA and 0.3% Triton™ X-100. Myotube cells treated with palmitic acid were significantly atrophied, compared with the control (Figure S3A). In addition, the fluorescence intensities of myosin heavy chain in palmitic acid-treated C2C12 myotube cells were significantly lower than those of control cells (Figure S3B). Moreover, the fusion index of C2C12 cells treated with palmitic acid was



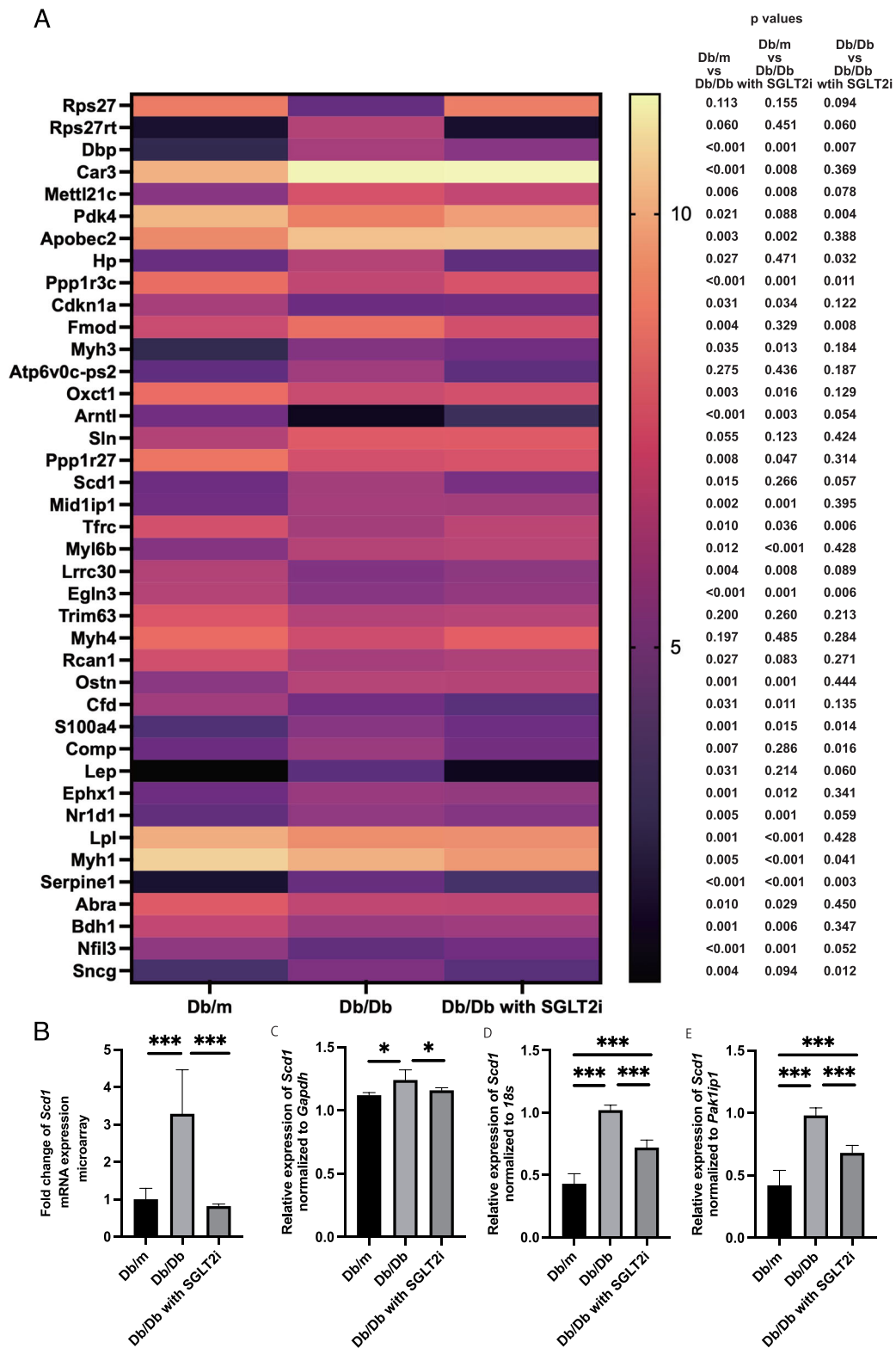


**Figure 4** Gene expression in muscle and annotation. (A) The  $\log_2(\text{FPKM} + 1)$  of the top 30 genes by the weighted average distance method was visualized in heat maps. *P*-values were shown. (B) Fold change of *Scd1* mRNA expression in microarray ( $n = 6$ ). (C) Relative expression of *Scd1* normalized *Gapdh* ( $n = 6$ ). (D) Relative expression of *Scd1* normalized *18s* ( $n = 6$ ). (E) Relative expression of *Scd1* normalized *Pak1ip1* ( $n = 6$ ). Data are presented as mean  $\pm$  standard deviation. \* $P < 0.05$  and \*\*\* $P < 0.001$ , using Tukey's honestly significant difference test.

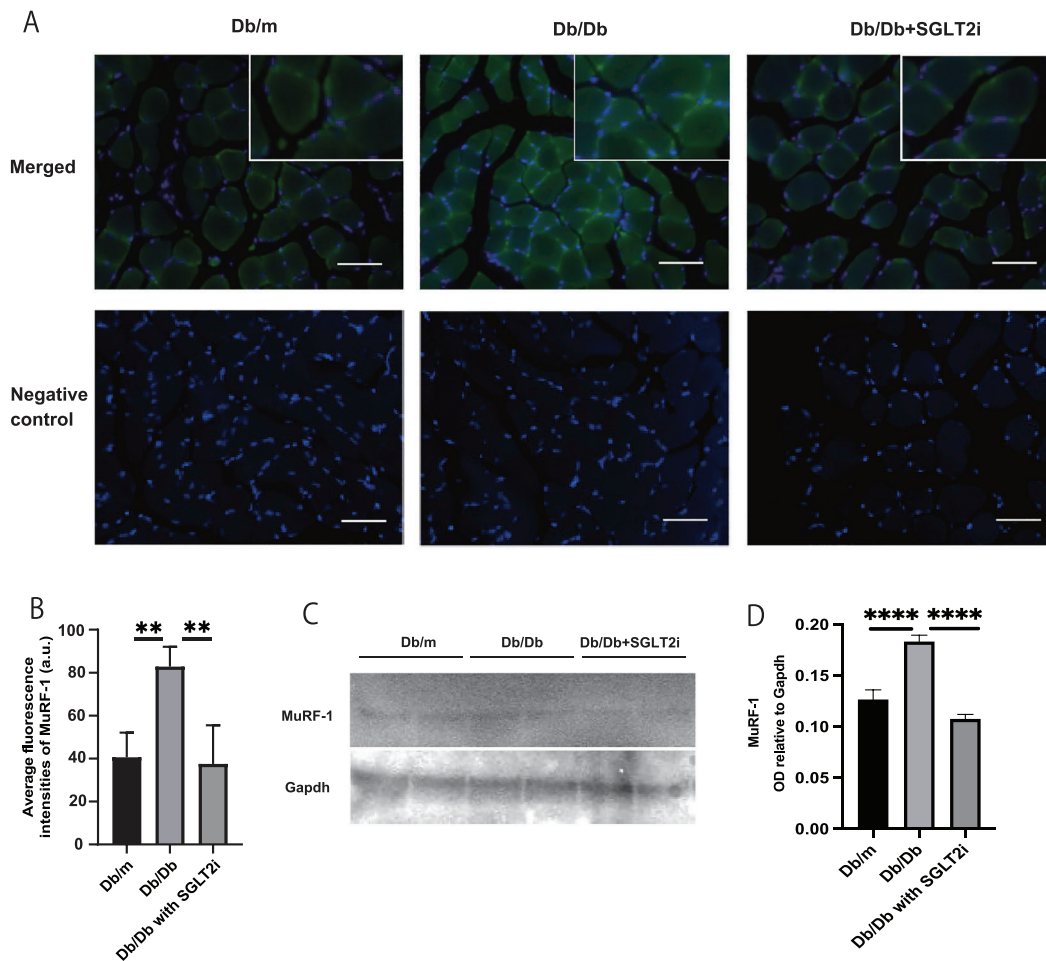


**Figure 5** SGLT2i reduces the expression intensity of MuRF1 in soleus muscle tissues. (A) Immunohistochemistry of soleus muscle tissues. Green: MuRF1, Blue: DAPI. Scale bar, 50  $\mu$ m. Upper: merged, lower: negative control. (B) The fluorescence intensity of MuRF1 ( $n = 6$ ). (C) Western blotting of MuRF-1 and Gapdh in soleus muscle. (D) The relative optical density (OD) of MuRF-1 to Gapdh ( $n = 6$ ). Data are presented as mean  $\pm$  standard deviation.  $**P < 0.01$  and  $****P < 0.0001$ , using Tukey's honestly significant difference test.

significantly lower than that of control cells (Figure S3D). On the other hand, the fluorescence intensities of MuRF1 in palmitic acid-treated C2C12 myotube cells were significantly higher than those of control cells (Figure S3A and S3C). Furthermore, in western blotting, the increase of MuRF1 and decreased of myosin heavy chain protein content occurred in C2C12 myotube cells treated with palmitic acid, compared with that of control (Figure S3E).

### Palmitic acid induces the expression of genes related to fatty acid metabolism and muscle atrophy in C2C12 myotube cells

Comparative threshold values of *Gapdh* were not significantly different between control C2C12 myotube cells and those treated with palmitic acid (Figure 6A). The gene expression levels of *Foxo1*, *Mstn*, *Hdac4*, *Trim63*, and *Fbxo32* in C2C12 myotube cells treated with palmitic acid were significantly

higher than those in control cells (Figure 6B–6F). Moreover, the expression levels of *Scd1*, *Fasn*, *Srebf1*, and *Elovl6*, genes related to fatty acid metabolism, were significantly increased in C2C12 myotube cells treated with palmitic acid, compared with those in control cells (Figure 6G–6J). Similarly, the expression of genes related to inflammation, *Il6*, and apoptosis, *Bax*, was significantly increased in C2C12 myotube cells treated with palmitic acid, with respect to control cells (Figure 6K and 6L).

## Discussion

In the present study, we administered SGLT2i to *db/db* mice and observed improved fatty acid metabolism, including reduced concentrations of saturated fatty acids in skeletal muscle as well as in serum. On the other hand, elevated levels of palmitic acid in the sera or liver of *db/db* mice might

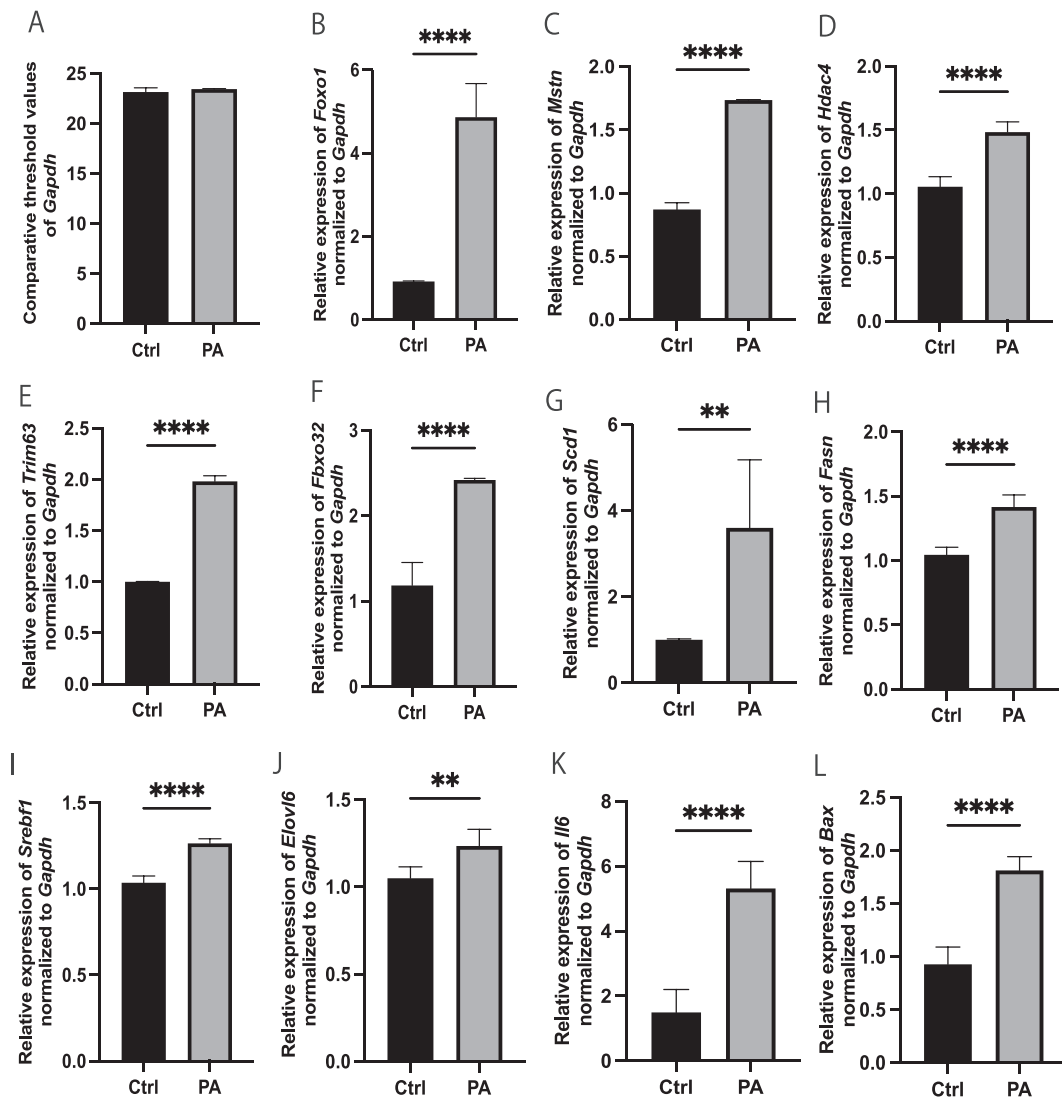


**Figure 6** Palmitic acid increases the expression of genes associated with muscle atrophy, fatty acid synthesis, inflammation, and apoptosis. (A) Comparative threshold values of *Gapdh* ( $n = 6$ ). Relative expression of indicated genes in C2C12 myotube cells normalized to *Gapdh*. (B) *Foxo1*, (C) *Mstn*, (D) *Hdac4*, (E) *Trim63*, (F) *Fbxo32*, (G) *Scd1*, (H) *Fasn*, (I) *Sreb1*, (J) *Elovl6*, (K) *Il6*, and (L) *Bax* ( $n = 6$ ). Data are presented as mean  $\pm$  standard deviation. \*\* $P < 0.01$  and \*\*\*\* $P < 0.0001$ , using an unpaired *t*-test.

lead to increased accumulation of palmitic acid in the skeletal muscle of *db/db* mice.

The microarray FPKM results also showed that the expression of *Cd36* was significantly decreased by SGLT2i treatment. It has been reported that CD36 can increase the rate of FA uptake by promoting intracellular metabolism, that is, esterification, without catalysing the translocation of FA across the cell membrane, and that CD36 plays a central role in FA uptake through its effects on intracellular metabolism.<sup>22</sup> The concentration of saturated fatty acids in skeletal muscle cells via Cd36, a fatty acid transporter on the surface of skeletal muscle cells, was decreased by SGLT2i treatment (Figure S4).<sup>23</sup> These saturated fatty acids are metabolized to acyl-CoA, which is then taken up by

mitochondria and metabolized through the tricarboxylic acid cycle. However, in *db/db* mice, the large amount of palmitic acid entering myocytes might not be fully metabolized within the tricarboxylic acid cycle. Moreover, malonyl-CoA released from the tricarboxylic acid cycle can also be converted to palmitic acid by the fatty acid synthase FAS. On the other hand, palmitic acid can also be converted to stearic acid by ELOVL6. Consistently, in *db/db* mice, the concentration of stearic acid increased in both serum and skeletal muscle.

In addition, oleic acid levels were elevated in *db/db* mice administered with SGLT2i, in both serum and skeletal muscle. Such increase of oleic acid concentration in the sera and liver might be due to an increase in the influx

of oleic acid into skeletal muscle cells. As a result, intracellular levels of palmitic acid decreased while intracellular levels of oleic acid increased in *db/db* mice treated with SGLT2i.

Furthermore, high concentrations of intramuscular palmitic acid are thought to exert lipotoxicity.<sup>24,25</sup> In the present study, an *in vitro* assay confirmed the lipotoxicity of palmitic acid. In fact, we demonstrated that palmitic acid treatment promoted the expression of muscle atrophy-associated genes, inflammatory cytokine, and apoptosis-associated genes in C2C12 myotubes. Stearic acid has been also reported to enhance insulin resistance in skeletal muscle cells.<sup>26</sup> In the same study, Hirabara *et al.* showed that stearic acid, same as palmitic acid, causes the decrease of insulin-stimulated glucose metabolism in skeletal muscle cells, which is mainly related to mitochondrial dysfunction. On the other hand, oleic acid has been reported to induce AMPK $\alpha$  phosphorylation and GPR43 protein abundance, thereby stimulating the differentiation of myotube cells.<sup>27,28</sup> These results suggest that not only the increase in palmitic acid concentration in skeletal muscle but also the decrease in oleic acid concentration may have played a key role in the preventive effect of SGLT2i on muscle atrophy in this study. Monounsaturated fatty acids are abundant in olive oil, and oleic acid is a typical example. Oleic acid interferes with pyroptosis, an inflammatory cell death and endoplasmic reticulum stress caused by saturated fatty acids, which are highly lipotoxic.<sup>29</sup> It has been reported that a diet rich in monounsaturated fatty acids reduces the risk of heart disease and is effective in treatment of NAFLD and type 2 diabetes.<sup>30–32</sup> There is no previous report on the relationship between SGLT2 inhibitors and oleic acid concentration in the liver; however, Shiba *et al.*<sup>33</sup> reported that canagliflozin, an SGLT2 inhibitor, significantly reduced hepatic fat deposition and TG content by lowering the expression of *de novo* lipogenic genes such as *scd1*. Therefore, we hypothesized that the increase of oleic acid in the liver by SGLT2i might cause down-regulation of *Scd1*.

SGLT2is modify the systemic lipidome as well as the serum lipidome in several ways.<sup>34–36</sup> Consistently, in the present study, we observed a decrease in the serum concentrations of saturated fatty acids. The modulation of the serum lipidome, especially the decrease in palmitic acid levels and the increase in oleic acid levels, is thought to affect the modulation of the intracellular lipidome. Therefore, because skeletal muscle cells do not express SGLT2 receptors,<sup>37</sup> we hypothesized that the modulation of the intra-skeletal muscle lipidome would occur mainly in conjunction with these changes in the serum lipidome. Taken together, our results showed that SGLT2i treatment reduced palmitic acid content and increased oleic acid content of skeletal muscle by altering the serum fatty acid profile, suggesting that SGLT2i might reduce lipotoxicity in skeletal muscle and, conversely, promote skeletal muscle differentiation.

In the present study, the concentration of palmitic acid, a saturated fatty acid, was found to increase in the skeletal muscle of *Db/Db* mice. These changes in the fatty acid profile of skeletal muscle were induced by SGLT2i administration, and decreased expression of *Scd1*, among genes related to fatty acid synthesis, was observed. It has been previously reported that elevated *Scd1* expression contributes to the progression of abnormal lipid metabolism and obesity.<sup>38</sup> Therefore, we believe that elevated levels of palmitate in skeletal muscle cells induce the expression of skeletal muscle atrophy-related genes, although the mechanism has not yet been fully elucidated.

In addition, the present study confirmed the benefits of SGLT2i administration, which not only improved fatty acid metabolism but also increased skeletal muscle weight and grip strength, resulting in the amelioration of sarcopenia. These findings are consistent with previous reports, showing that abnormalities in lipid metabolism in skeletal muscle may exacerbate sarcopenia.<sup>39,40</sup> On the other hand, the increase in grip strength by SGLT2i has been reported only once in Japanese patients with type 2 diabetes,<sup>41</sup> and this is the first study that revealed the increase in grip strength in animal experiments. Taken together, our results demonstrated that SGLT2i improved fatty acid metabolism, modifying the fatty acid composition of serum and skeletal muscle. In particular, we suggest that reduced fatty acid accumulation within skeletal muscle might lead to a decreased lipotoxicity and to the mitigation of sarcopenia.

As a limitation of this study, the microarray results are shown in FPKM; however, it has been reported that FPKM does not correctly represent the expression level of transcripts,<sup>42</sup> and recently, TPM has been used instead of FPKM. In the future, the results of the microarray should be presented in TPM.

In conclusion, SGLT2i administration inhibited the atrophy of skeletal muscle cells, although these do not express SGLT2 receptors. We hypothesized that the promotion of urinary excretion of glucose by SGLT2i would result in decreased serum glucose and palmitic acid concentrations and, in parallel, in decreased palmitic acid concentrations and increased unsaturated fatty acid concentrations in skeletal muscle cells. Along with these modified fatty acid levels in skeletal muscle cells, we found reduced expression of genes, such as *Fasn*, *Elovl6*, and *Scd1*, involved in fatty acid synthesis. Based on these findings, we hypothesized that secondary effects, other than the hypoglycaemic effects of SGLT2i, might lead to the alleviation of obesity-dependent sarcopenia.

## Acknowledgements

We thank all staff members of the Kyoto Prefectural University of Medicine.

## Conflict of interest

Y.H. received grants from Asahi Kasei Pharma, personal fees from Daiichi Sankyo Co., Ltd., personal fees from Mitsubishi Tanabe Pharma Corp., personal fees from Sanofi K.K., and personal fees from Novo Nordisk Pharma Ltd., outside the submitted work. T.S. received personal fees from Ono Pharma Co., Ltd., Mitsubishi Tanabe Pharma Co., Astellas Pharma Inc., Kyowa Hakko Kirin Co., Ltd., Sanofi K.K., MSD K.K., Kowa Pharma Co., Ltd., Taisho Toyama Pharma Co., Ltd., Takeda Pharma Co., Ltd., Kissei Pharma Co., Ltd., Novo Nordisk Pharma Ltd., and Eli Lilly Japan K.K. outside the submitted work. E.U. received grants from the Japanese Study Group for Physiology and Management of Blood Pressure and the Astellas Foundation for Research on Metabolic Disorders (Grant Number: 4024). The Donated Fund Laboratory of Diabetes Therapeutics is an endowment department, supported by an unrestricted grant from Ono Pharmaceutical Co., Ltd., and received personal fees from AstraZeneca plc, Astellas Pharma Inc., Daiichi Sankyo Co., Ltd., Kyowa Hakko Kirin Company Ltd., Kowa Pharmaceutical Co., Ltd., MSD K.K., Mitsubishi Tanabe Pharma Corp., Novo Nordisk Pharma Ltd., Taisho Toyama Pharmaceutical Co., Ltd., Takeda Pharmaceutical Co., Ltd., Nippon Boehringer Ingelheim Co., Ltd., and Sumitomo Dainippon Pharma Co., Ltd., outside the submitted work. M.H. received grants from Asahi Kasei Pharma, Nippon Boehringer Ingelheim Co., Ltd., Mitsubishi Tanabe Pharma Corporation, Daiichi Sankyo Co., Ltd., Sanofi K.K., Takeda Pharmaceutical Company Limited, Astellas Pharma Inc., Kyowa Kirin Co., Ltd., Sumitomo Dainippon Pharma Co., Ltd., Novo Nordisk Pharma Ltd., and Eli Lilly Japan K.K., outside the submitted work. M.A. received personal fees from Novo Nordisk Pharma Ltd., Abbott Japan Co., Ltd., AstraZeneca plc, Kowa Pharmaceutical Co., Ltd., Ono Pharmaceutical Co., Ltd., and Takeda Pharmaceutical Co., Ltd., outside the submitted work. M.Y. reports personal fees from MSD K.K., Sumitomo Dainippon Pharma Co., Ltd., Kowa Company, Limited, AstraZeneca PLC, Takeda Pharmaceutical Company Limited, Kyowa Hakko Kirin Co., Ltd., Daiichi Sankyo Co., Ltd., Kowa Pharmaceutical Co., Ltd., and Ono Pharma Co., Ltd., outside the submitted work. M.F. received grants from Nippon Boehringer Ingelheim Co., Ltd., Kissei Pharma Co., Ltd., Mitsubishi Tanabe Pharma Co., Daiichi Sankyo Co., Ltd., Sanofi K.K., Takeda Pharma Co., Ltd., Astellas Pharma Inc., MSD K.K., Kyowa Hakko Kirin Co., Ltd., Sumitomo Dainippon Pharma Co., Ltd., Kowa Pharmaceutical Co., Ltd., Novo Nordisk Pharma Ltd., Ono Pharma Co., Ltd., Sanwa Kagaku Kenkyusho Co., Ltd., Eli Lilly Japan K.K., Taisho Pharma Co., Ltd., Terumo Co., Teijin Pharma Ltd., Nippon Chemiphar Co., Ltd., Johnson & Johnson K.K. Medical Co., and Abbott Japan Co., Ltd. and received personal fees from Nippon Boehringer Ingelheim Co., Ltd., Kissei Pharma Co., Ltd., Mitsubishi Tanabe Pharma Corp., Daiichi Sankyo Co., Ltd., Sanofi K.K., Takeda Pharma Co., Ltd., Astellas Pharma

Inc., MSD K.K., Kyowa Kirin Co., Ltd., Sumitomo Dainippon Pharma Co., Ltd., Kowa Pharma Co., Ltd., Novo Nordisk Pharma Ltd., Ono Pharma Co., Ltd., Sanwa Kagaku Kenkyusho Co., Ltd., Eli Lilly Japan K.K., Taisho Pharma Co., Ltd., Bayer Yakuhin, Ltd., AstraZeneca K.K., Mochida Pharma Co., Ltd., Abbott Japan Co., Ltd., Medtronic Japan Co., Ltd., Arkley Inc., Teijin Pharma Ltd., and Nipro Cor., outside the submitted work.

## Funding

This research received funding from Taisho Pharmaceutical Co., Ltd.

## Online supplementary material

Additional supporting information may be found online in the Supporting Information section at the end of the article.

**Figure S1.** SGLT2i decreases hepatic fat accumulation and fibrosis.

**A:** Representative images showing the histological features of the liver. **B:** NAFLD activity score ( $n = 6$ ). **C:** NAS fibrosis stage ( $n = 6$ ). **D:** lauric, **E:** myristic, **F:** palmitic, **G:** stearic, and **H:** oleic acid concentration ( $n = 6$ ). Data are presented as mean  $\pm$  SD.  $*p < 0.05$ ,  $**p < 0.01$ , and  $***p < 0.001$ , using Tukey's HSD test.

**Figure S2.** Volcano plots representing changes in gene expression

Volcano plots show the estimated fold changes (x-axis) against the  $-\log_{10} p$  values (y-axis).

**A:** *db/db* mice/ *db/m* mice. **B:** *db/db* mice treated with SGLT2i/*db/m* mice. **C:** *db/db* mice treated with SGLT2i/*db/db* mice.

**Figure S3.** Palmitic acid induces atrophy in C2C12 myotube cells

**A:** Immunohistochemistry of control (Ctrl) and palmitic acid (PA)-treated C2C12 myotube cells. Green: Myosin heavy chain. Red: MuRF1. Blue: DAPI. Scale bar, 100  $\mu$ m. The fluorescence intensities of **B:** myosin heavy chain and **C:** MuRF1 expressed in an arbitrary unit (a.u.) were compared. **D:** Fusion index of C2C12 myotube cells. **E:** Western blotting of MuRF-1 and Gapdh in C2C12 myotube cells.

Data are presented as mean  $\pm$  SD;  $*p < 0.05$ ,  $**p < 0.01$ , and  $***p < 0.001$ , using an unpaired t-test.

**Figure S4.** Comparison of lipid metabolite levels and gene expression in skeletal muscle of *db/db* mice with or without SGLT2i treatment

Gene expressions are fold changes of mRNA expression in microarray ( $n = 6$ ).

Data are presented as mean  $\pm$  SD;  $*p < 0.05$ ,  $**p < 0.01$ ,  $***p < 0.001$ , and  $****p < 0.0001$  using an unpaired t-test.



## References

- Saeedi P, Petersohn I, Salpea P, Malanda B, Karuranga S, Unwin N, et al. Global and regional diabetes prevalence estimates for 2019 and projections for 2030 and 2045: results from the International Diabetes Federation Diabetes Atlas, 9th edition. *Diabetes Res Clin Pract* 2019;**157**:107843.
- Bolinder J, Ljunggren O, Johansson L, Wilding J, Langkilde AM, Sjöström CD, et al. Dapagliflozin maintains glycaemic control while reducing weight and body fat mass over 2 years in patients with type 2 diabetes mellitus inadequately controlled on metformin. *Diabetes Obes Metab* 2014;**16**:159–169.
- Abdul-Ghani M, Del Prato S, Chilton R, De Fronzo RA. SGLT2 inhibitors and cardiovascular risk: lessons learned from the EMPA-REG Outcome study. *Diabetes Care* 2016;**39**:717–725.
- Perkovic V, de Zeeuw D, Mahaffey KW, Fulcher G, Erondou N, Shaw W, et al. Canagliflozin and renal outcomes in type 2 diabetes: results from the CANVAS Program randomised clinical trials. *Lancet Diabetes Endocrinol* 2018;**6**:691–704.
- Cai X, Yang W, Gao X, Chen Y, Zhou L, Zhang S, et al. The association between the dosage of SGLT2 inhibitor and weight reduction in type 2 diabetes patients: a meta-analysis. *Obesity* 2018;**26**:70–80.
- Sasaki T. Sarcopenia, frailty circle and treatment with sodium–glucose cotransporter 2 inhibitors. *J Diabetes Investig* 2019;**10**:193–195.
- Kim KM, Jang HC, Lim S. Differences among skeletal muscle mass indices derived from height-, weight-, and body mass index-adjusted models in assessing sarcopenia. *Korean J Intern Med* 2016;**31**:643–650.
- Okamura T, Hashimoto Y, Osaka T, Fukuda T, Hamaguchi M, Fukui M. The sodium-glucose cotransporter 2 inhibitor luseogliflozin can suppress muscle atrophy in Db/Db mice by suppressing the expression of *foxo1*. *J Clin Biochem Nutr* 2019;**65**:23–28.
- Schenk S, Horowitz JF. Acute exercise increases triglyceride synthesis in skeletal muscle and prevents fatty acid-induced insulin resistance. *J Clin Invest* 2007;**117**:1690–1698.
- Kelley DE, Goodpaster B, Wing RR, Simoneau JA. Skeletal muscle fatty acid metabolism in association with insulin resistance, obesity, and weight loss. *Am J Physiol Endocrinol Metab* 1999;**277**:E1130–E1141.
- Dyck DJ, Heigenhauser GJF, Bruce CR. The role of adipokines as regulators of skeletal muscle fatty acid metabolism and insulin sensitivity. *Acta Physiologica* 2006;**186**:5–16.
- Marcus RL, Addison O, Dibble LE, Foreman KB, Morrell G, Lastayo P. Intramuscular adipose tissue, sarcopenia, and mobility function in older individuals. *J Aging Res* 2012;**2012**:629637.
- Kawai S, Takagi Y, Kaneko S, Kurosawa T. Effect of three types of mixed anesthetic agents alternate to ketamine in mice. *Exp Anim* 2011;**60**:481–487.
- Kleiner DE, Brunt EM, van Natta M, Behling C, Contos MJ, Cummings OW, et al. Design and validation of a histological scoring system for nonalcoholic fatty liver disease. *Hepatology* 2005;**41**:1313–1321.
- Okamura T, Hamaguchi M, Bamba R, Nakajima H, Yoshimura Y, Kimura T, et al. Immune modulating effects of additional supplementation of estradiol combined with testosterone in murine testosterone-deficient NAFLD model. *Am J Physiol Gastrointest Liver Physiol* 2020;**318**:G989–G999.
- Kadota K, Nakai Y, Shimizu K. A weighted average difference method for detecting differentially expressed genes from microarray data. *Algorithms Mol Biol* 2008;**3**:8.
- Roberts A, Trapnell C, Donaghey J, Rinn JL, Pachter L. Improving RNA-Seq expression estimates by correcting for fragment bias. *Genome Biol* 2011;**12**:R22.
- Livak KJ, Schmittgen TD. Analysis of relative gene expression data using real-time quantitative PCR and the  $2^{-\Delta\Delta CT}$  method. *Methods* 2001;**25**:402–408.
- Widner DB, Liu C, Zhao Q, Sharp S, Eber MR, Park SH, et al. Activated mast cells in skeletal muscle can be a potential mediator for cancer-associated cachexia. *J Cachexia Sarcopenia Muscle* 2021;**12**:1079–1097.
- Yamaguchi T, Suzuki T, Arai H, Tanabe S, Atomi Y. Continuous mild heat stress induces differentiation of mammalian myoblasts, shifting fiber type from fast to slow. *Am J Physiol Cell Physiol* 2010;**298**:C140–C148.
- Matsui H, Yokoyama T, Sekiguchi K, Iijima D, Sunaga H, Maniwa M, et al. Stearoyl-CoA desaturase-1 (SCD1) augments saturated fatty acid-induced lipid accumulation and inhibits apoptosis in cardiac myocytes. *PLoS ONE* 2012;**7**:e33283.
- Xu S, Jay A, Brunaldi K, Huang N, Hamilton JA. CD36 enhances fatty acid uptake by increasing the rate of intracellular esterification but not transport across the plasma membrane. *Biochemistry* 2013;**52**:7254–7261.
- Ibrahimi A, Bonen A, Blinn WD, Hajri T, Li X, Zhong K, et al. Muscle-specific overexpression of FAT/CD36 enhances fatty acid oxidation by contracting muscle, reduces plasma triglycerides and fatty acids, and increases plasma glucose and insulin. *J Biol Chem* 1999;**274**:26761–26766.
- Lee H, Lim JY, Choi SJ. Oleate prevents palmitate-induced atrophy via modulation of mitochondrial ROS production in skeletal myotubes. *Oxid Med Cell Longev* 2017;**2017**:273972.
- Henique C, Mansouri A, Fumey G, Lenoir V, Girard J, Bouillaud F, et al. Increased mitochondrial fatty acid oxidation is sufficient to protect skeletal muscle cells from palmitate-induced apoptosis. *J Biol Chem* 2010;**285**:36818–36827.
- Hirabara SM, Curi R, Maechler P. Saturated fatty acid-induced insulin resistance is associated with mitochondrial dysfunction in skeletal muscle cells. *J Cell Physiol* 2010;**222**:187–194.
- Lim JH, Gerhart-Hines Z, Dominy JE, Lee Y, Kim S, Tabata M, et al. Oleic acid stimulates complete oxidation of fatty acids through protein kinase A-dependent activation of SIRT1-PGC1 $\alpha$  complex. *J Biol Chem* 2013;**288**:7117–7126.
- Hurley MS, Flux C, Salter AM, Brameld JM. Effects of fatty acids on skeletal muscle cell differentiation in vitro. *Br J Nutr* 2006;**95**:623–630.
- Zeng X, Zhu M, Liu X, Chen X, Yuan Y, Li L, et al. Oleic acid ameliorates palmitic acid induced hepatocellular lipotoxicity by inhibition of ER stress and pyroptosis. *Nutr Metab* 2020;**17**:11.
- Morgan NG, Dhayal S. Unsaturated fatty acids as cytoprotective agents in the pancreatic B-cell. *Prostaglandins Leukot Essent Fatty Acids* 2010;**82**:231–236.
- Schwingshackl L, Strasser B, Hoffmann G. Effects of monounsaturated fatty acids on glycaemic control in patients with abnormal glucose metabolism: a systematic review and meta-analysis. *Ann Nutr Metab* 2011;**58**:290–296.
- de Barros CR, Cezaretto A, Curti MLR, Pires MM, Folchetti LD, Siqueira-Catania A, et al. Realistic changes in monounsaturated fatty acids and soluble fibers are able to improve glucose metabolism. *Diabetol Metab Syndr* 2014;**6**:136.
- Shiba K, Tsuchiya K, Komiya C, Miyachi Y, Mori K, Shimazu N, et al. Canagliflozin, an SGLT2 inhibitor, attenuates the development of hepatocellular carcinoma in a mouse model of human NASH. *Sci Rep* 2018;**8**:2362.
- Raj H, Durgina H, Palui R, Kamalanathan S, Selvarajan S, Kar SS, et al. SGLT-2 inhibitors in non-alcoholic fatty liver disease patients with type 2 diabetes mellitus: a systematic review. *World J Diabetes* 2019;**10**:114–132.
- Xu L, Ota T. Emerging roles of SGLT2 inhibitors in obesity and insulin resistance: focus on fat browning and macrophage polarization. *Adipocyte* 2018;**7**:121–128.
- Hawley SA, Ford RJ, Smith BK, Gowans GJ, Mancini SJ, Pitt RD, et al. The Na<sup>+</sup>/glucose cotransporter inhibitor canagliflozin activates AMPK by inhibiting mitochondrial function and increasing cellular AMP levels. *Diabetes* 2016;**65**:2784–2794.
- Wright EM, Loo DD, Hirayama BA. Biology of human sodium glucose transporters. *Physiol Rev* 2011;**91**:733–794.
- Hulver MW, Berggren JR, Carper MJ, Miyazaki M, Ntambi JM, Hoffman EP, et al. Elevated stearoyl-CoA desaturase-1 expression in skeletal muscle contributes to abnormal fatty acid partitioning in obese humans. *Cell Metab* 2005;**2**:251–261.

39. Zhou Q, Du J, Hu Z, Walsh K, Wang XH. Evidence for adipose-muscle cross talk: opposing regulation of muscle proteolysis by adiponectin and fatty acids. *Endocrinology* 2007;**148**:5696–5705.
40. Goodpaster BH, He J, Watkins S, Kelley DE. Skeletal muscle lipid content and insulin resistance: evidence for a paradox in endurance-trained athletes. *J Clin Endocrinol Metab* 2001;**86**:5755–5761.
41. Sano M, Meguro S, Kawai T, Suzuki Y. Increased grip strength with sodium-glucose cotransporter 2. *J Diabetes* 2016;**8**:736–737.
42. Wagner GP, Kin K, Lynch VJ. Measurement of mRNA abundance using RNA-seq data: RPKM measure is inconsistent among samples. *Theory Biosci* 2012;**131**: 281–285.